The Influence of Mixed-Phase Clouds on Surface Shortwave Irradiance During the Arctic Spring

Dan Lubin
Scripps Institution of Oceanography
UCSD, La Jolla, California, 92093, USA
Andrew M. Vogelmann
Brookhaven National Laboratory
Upton, New York, 11973, USA

Submitted to *Journal of Geophysical Research*, 01 February 2011
for the special section on the *Indirect and Semi-Direct Aerosol Campaign* (ISDAC)

Shortwave Surface Spectral Flux Measurements During ISDAC

ASD (Inc.) spectroradiometer at Great White recorded spectra every minute during Apr-May 2008 & Apr-Oct 2009.

- **Spectral coverage is 350-2200 nm.**
- **Resolution is 3 nm in VIS, 10 nm in NIR.**
- **Covers 1.6 and 2.2 micron windows, where spectral signature depends strongly on cloud microphysics.**

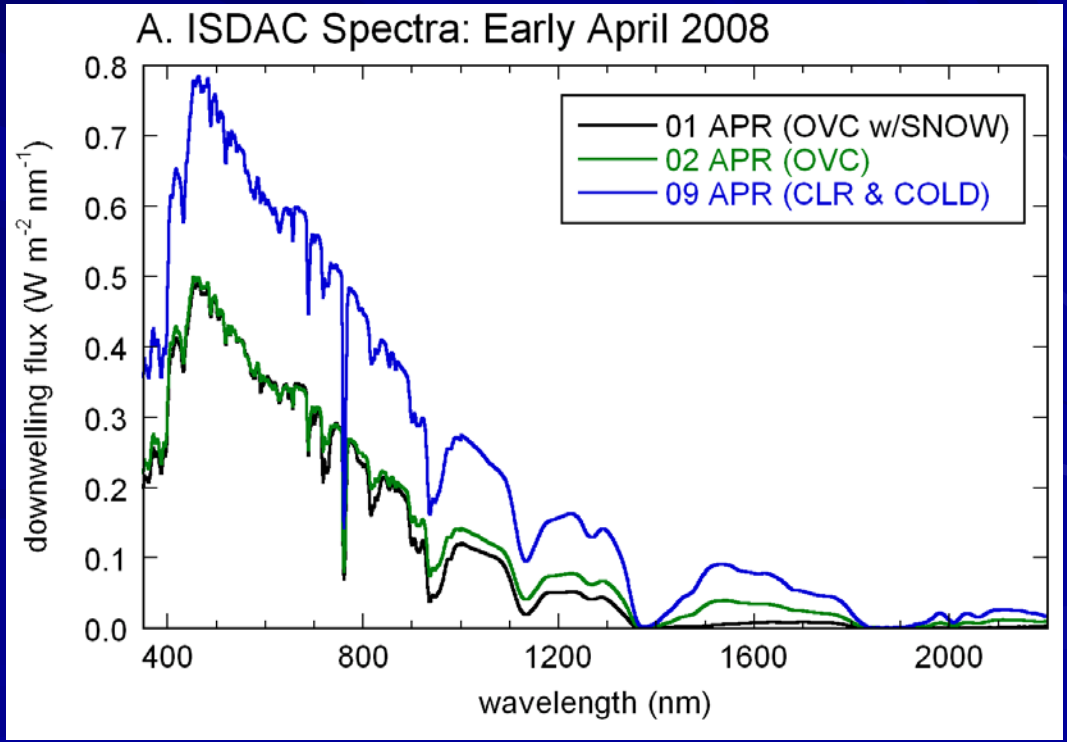

Theoretical Basis – Liquid Water Clouds

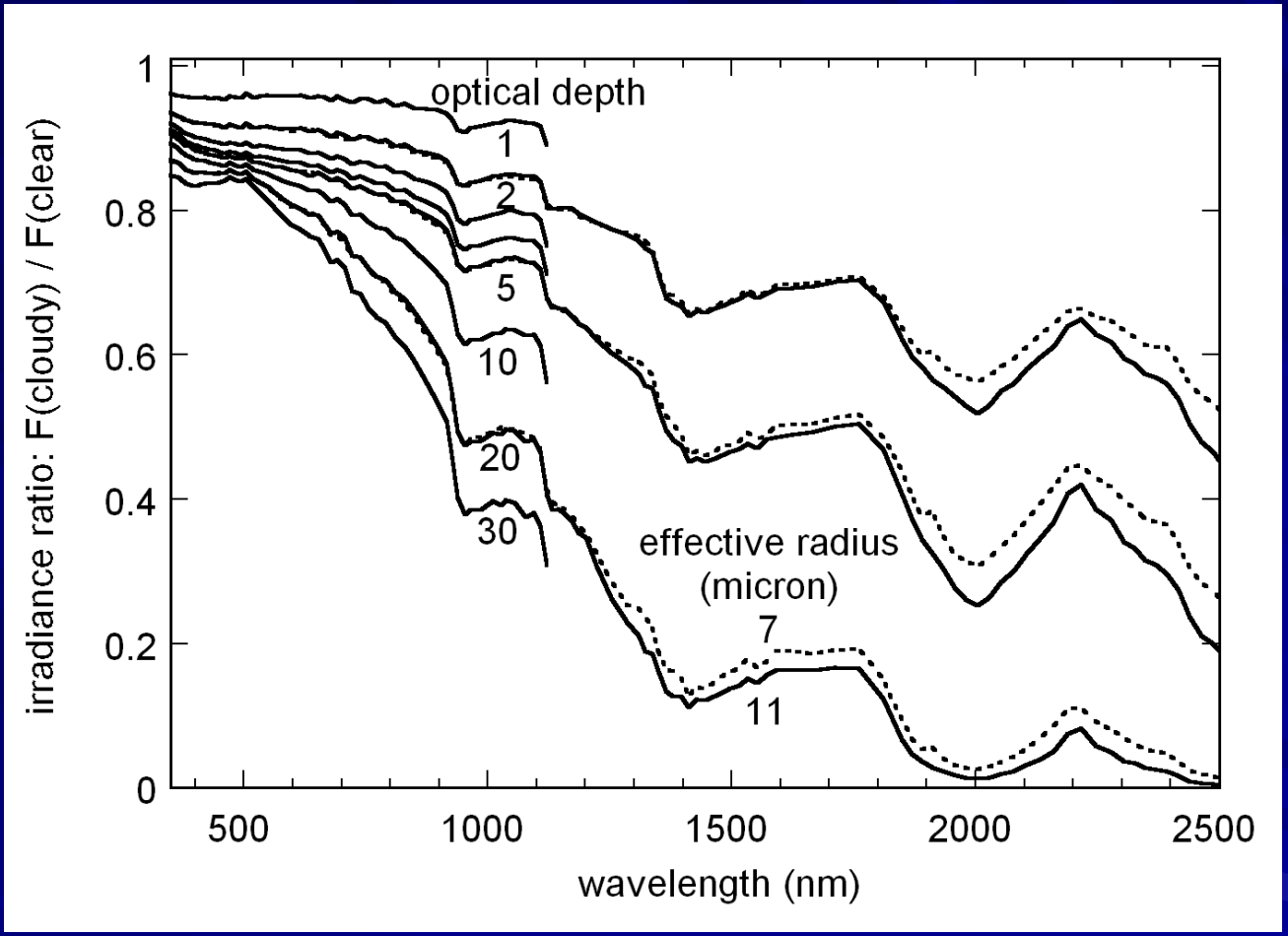

Figure 1. DISORT simulation of the spectral dependence of liquid water cloud attenuation of surface shortwave irradiance (relative to clear sky) as a function of cloud optical depth. The surface albedo is that of new snow, and the solar zenith angle 60^{o}. For clarity, only the curves for optical depths 2, 5, and 20 are fully shown. Solid and dotted curves depict the flux ratio for droplet effective radius 11 and 7 μm, respectively.

Surface Albedos
from Perovich et al. (2002; SHEBA)

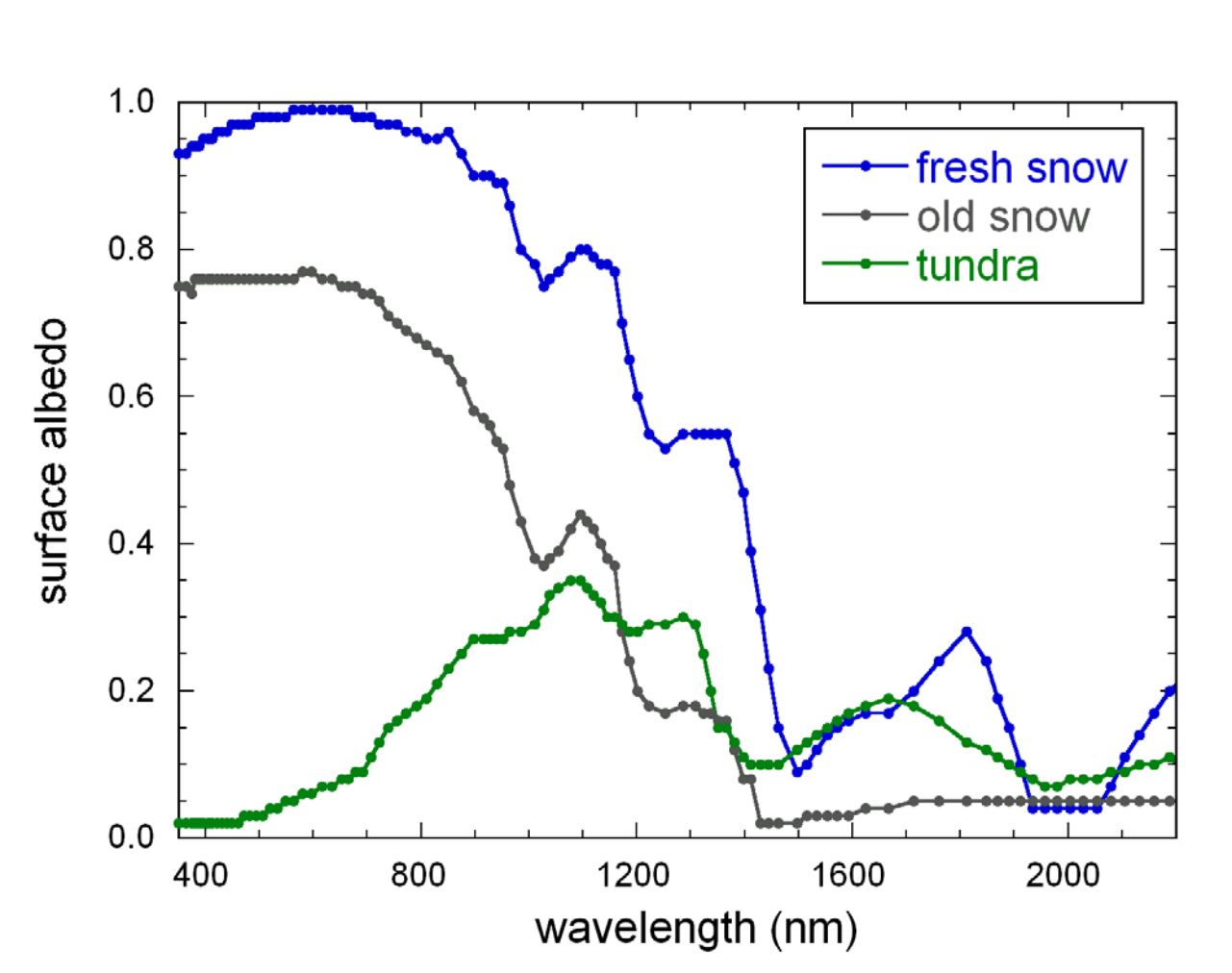

Theoretical Basis – Ice in Cloud

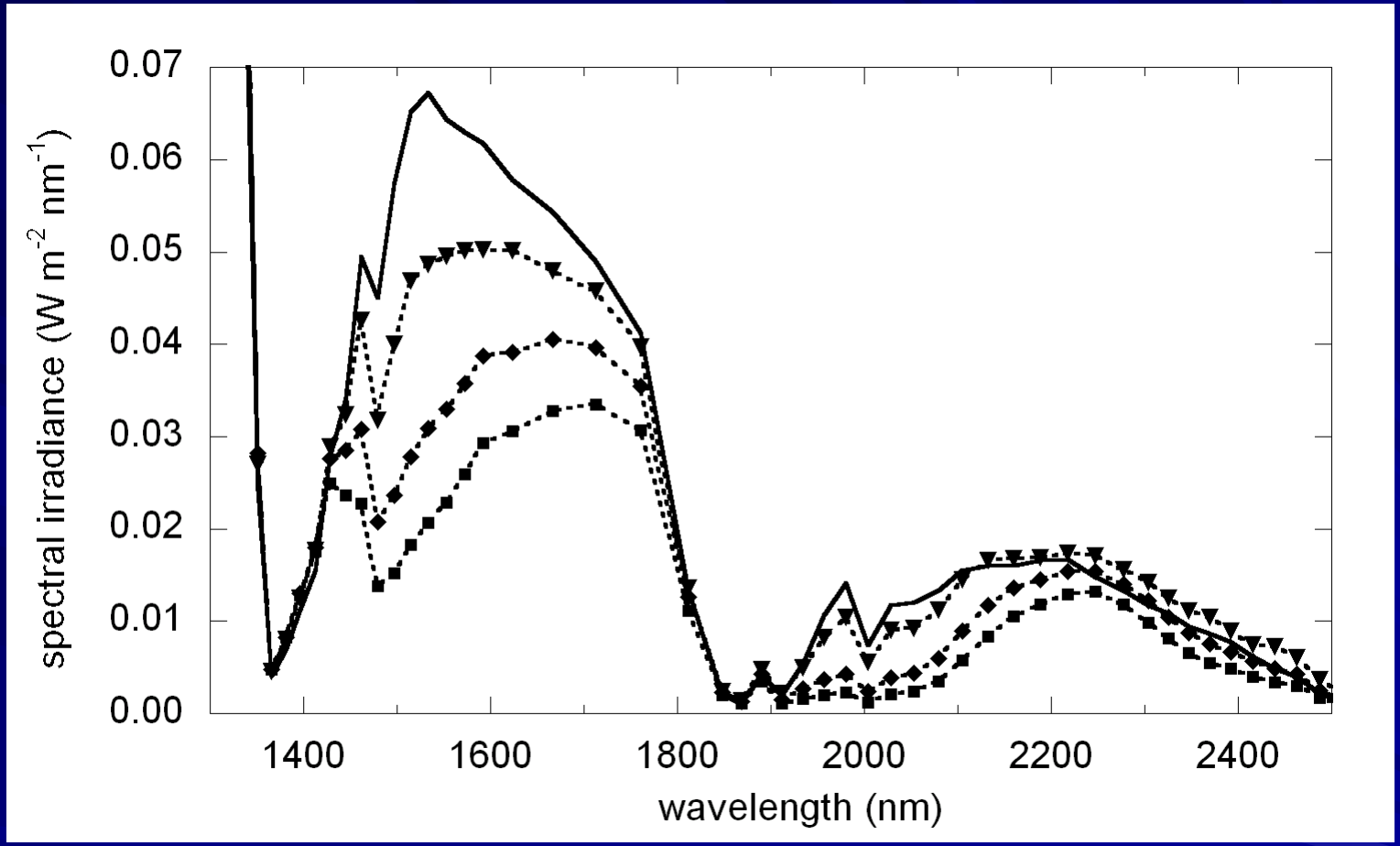

Figure 2. DISORT simulation of downwelling surface spectral irradiance in the 1.6 and 2.2 μm windows. The cloud optical depth (conservative scattering) is 5 over a new snow surface and the solar zenith angle is 60°. The liquid-water cloud has an effective radius 11 μm (solid curve), and the ice cloud has effective particle sizes of 10, 30, and 50 μm (triangles, diamonds, squares, respectively)

Mixed Phase Forcing

- We calculate a mixed-phase narrowband surface forcing, F_M, for each measured irradiance spectrum using a three-step process.
- In the first step, we determine the conservative-scattering cloud optical depth, τ_c, that matches the model-calculated surface irradiance with the measured surface irradiance in the 1022-1033 nm wavelength band.
- In the second step, we calculate a theoretical surface spectral irradiance using that value of τ_c and the same solar-illumination geometry, for a liquid-water cloud having an effective droplet radius of 11 μm.
- In the third step, we integrate over the 1.6 μm window (1374 - 1838 nm) both the modeled spectral irradiance under this liquid-water cloud and the measured spectral irradiance, and then subtract the measured value from the theoretical liquid-water-cloud value.

ISDAC “Golden Day” Example

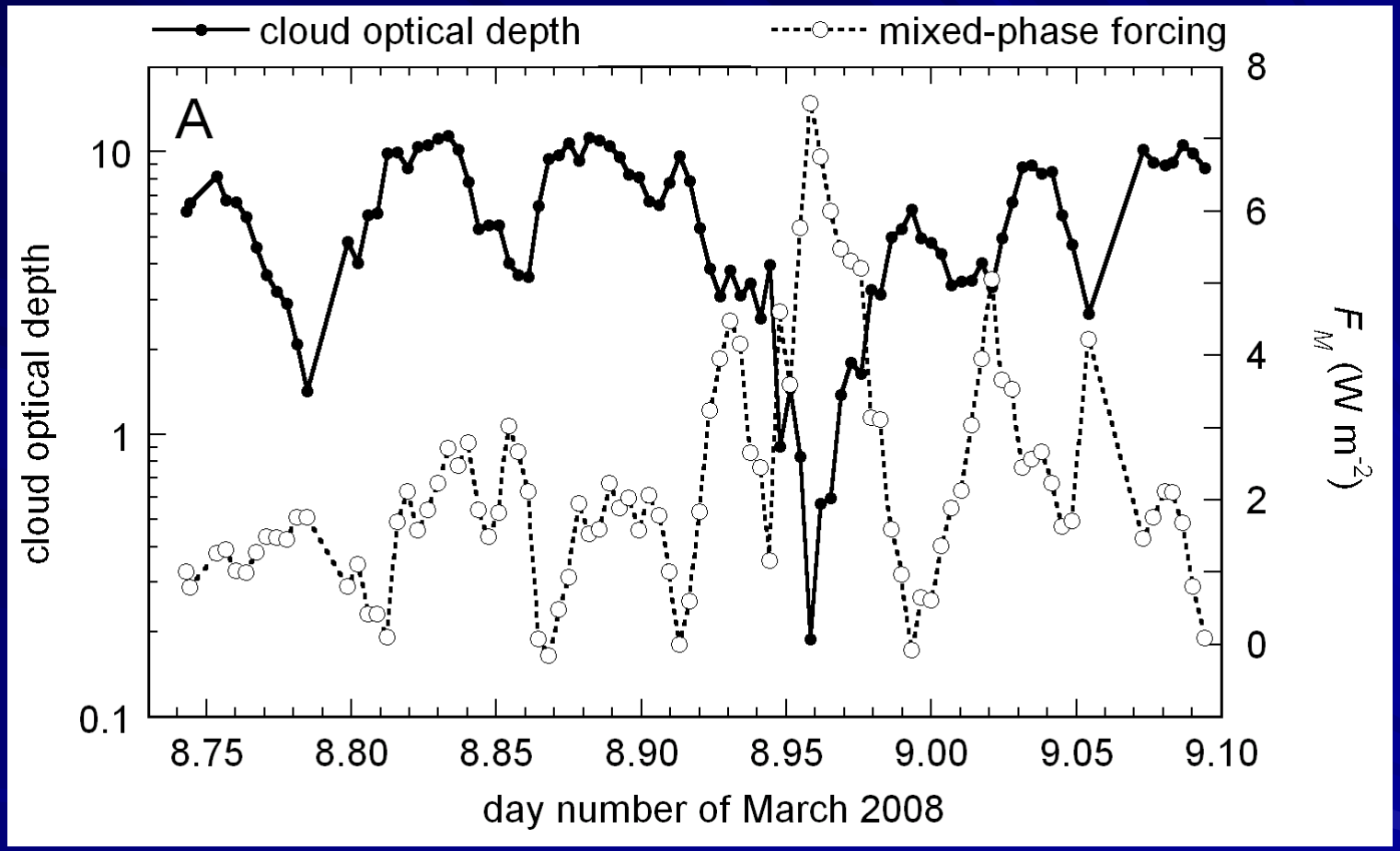

Figure 3. Time series of 5-minute-averaged cloud optical depth τc and mixed-phase surface forcing F_M in the 1.6-μm window, from the ISDAC "Golden Days" of 8 and 26 April, 2008

ISDAC “Golden Day” Example

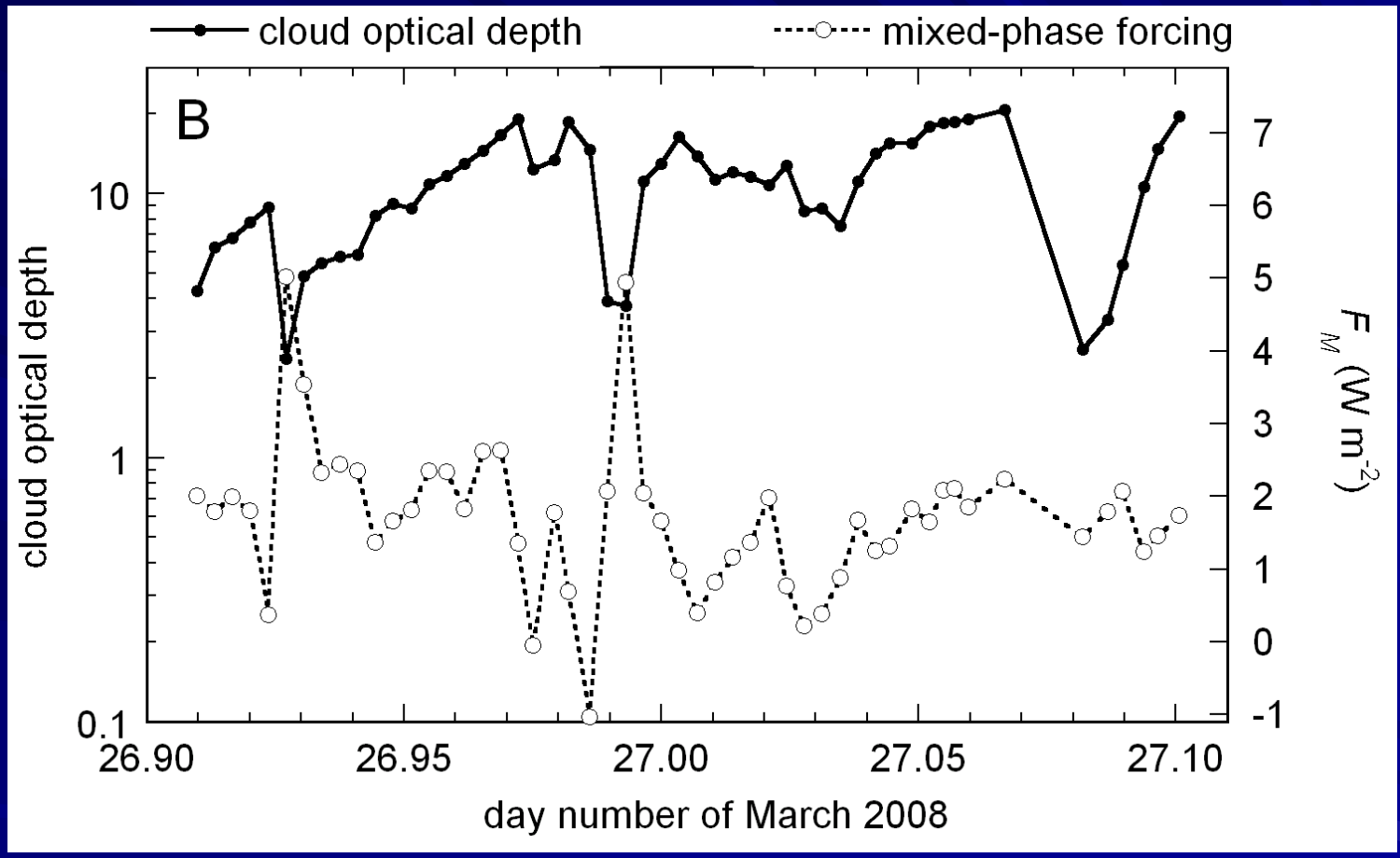

Figure 3. Time series of 5-minute-averaged cloud optical depth τc and mixed-phase surface forcing F_M in the 1.6-μm window, from the ISDAC "Golden Days" of 8 and 26 April, 2008

Cloud Geometrical Thickness from ARSCL

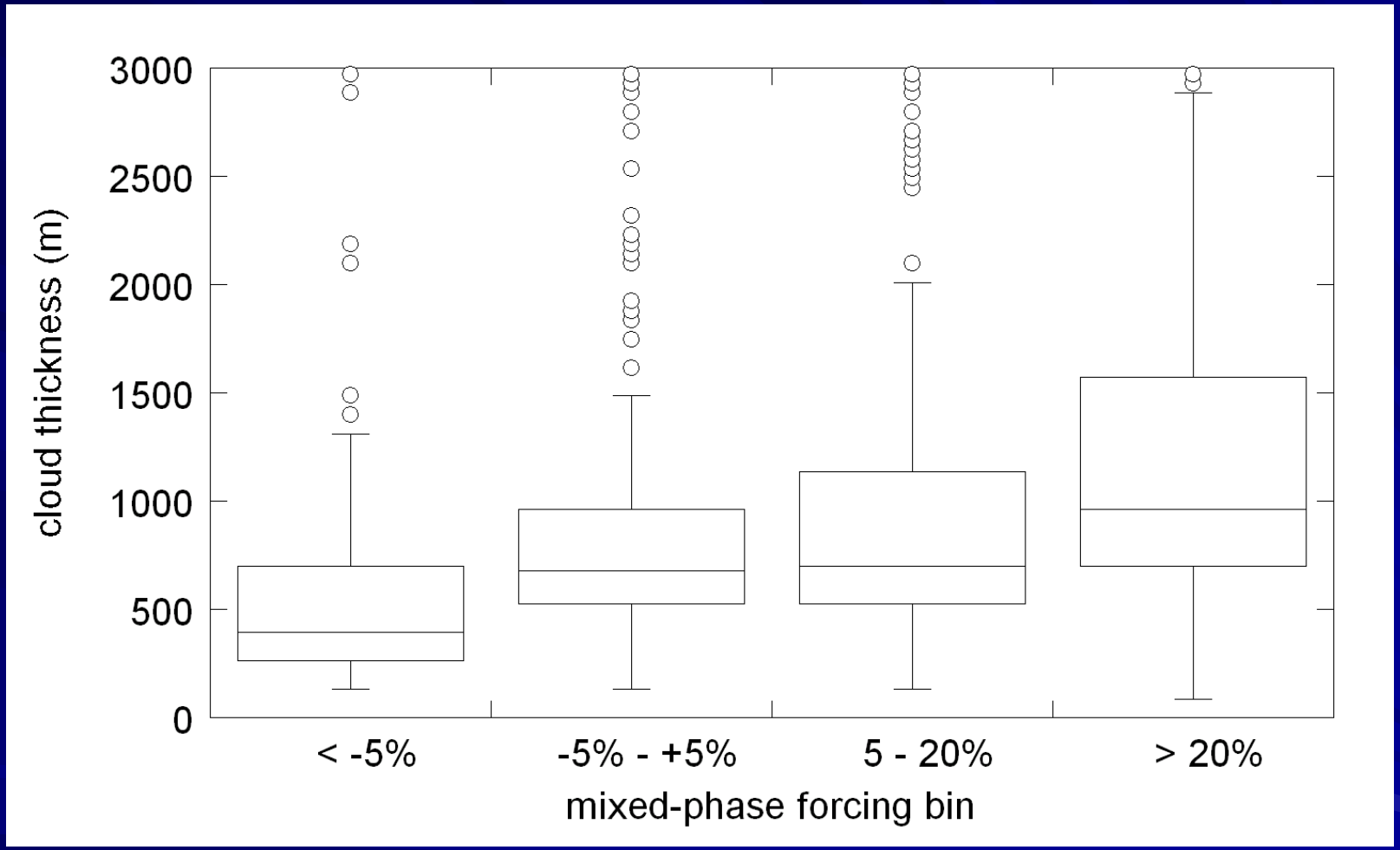

Figure 4. Box and whisker plot of ARSCL cloud thicknesses that prevailed during four general categories of mixed-phase surface forcing F_M described in the text. The line bisecting each box is the median; the box encompasses 50% of the interquartile distance (IQD), and the vertical bars depict the range ±1.5 IQD. Circles depict individual outliers.

Cloud Optical Depth

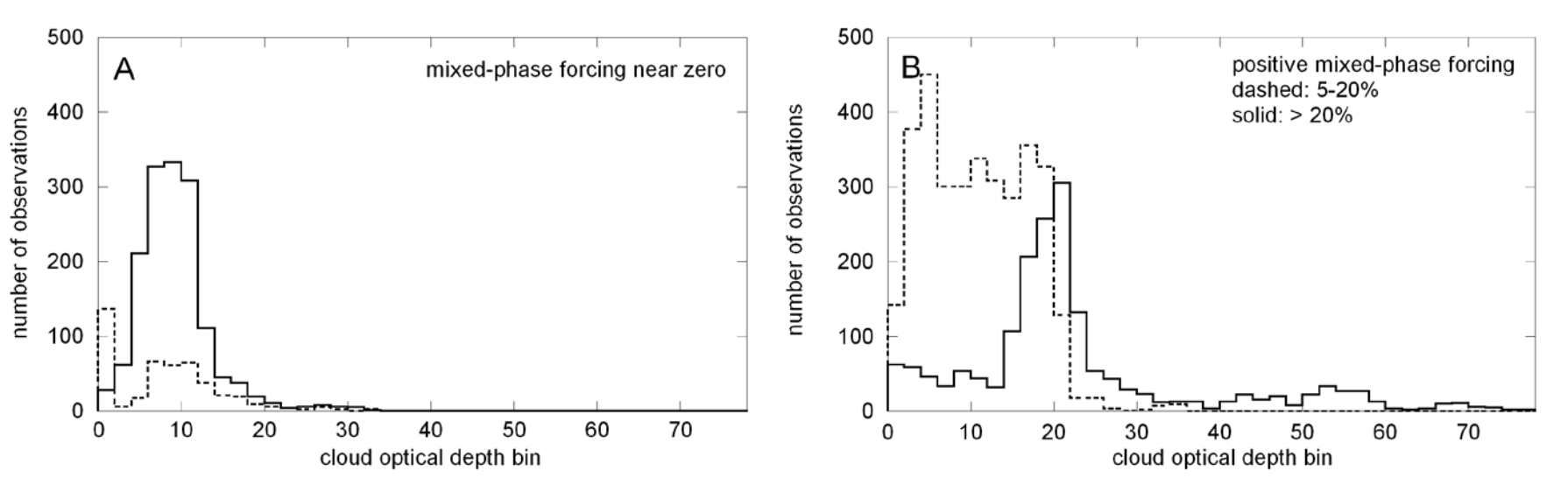

Figure 5. Histograms of cloud optical depth τc for the four general categories of mixed-phase surface forcing F_M described in the text: (A) for near-zero F_M (solid) and $F_M < -5\%$ (dashed); (B) $F_M \geq 20\%$ (solid) and $5\% \leq F_M < 20\%$ (dashed).

Cloud Effective Temperature from Sondes

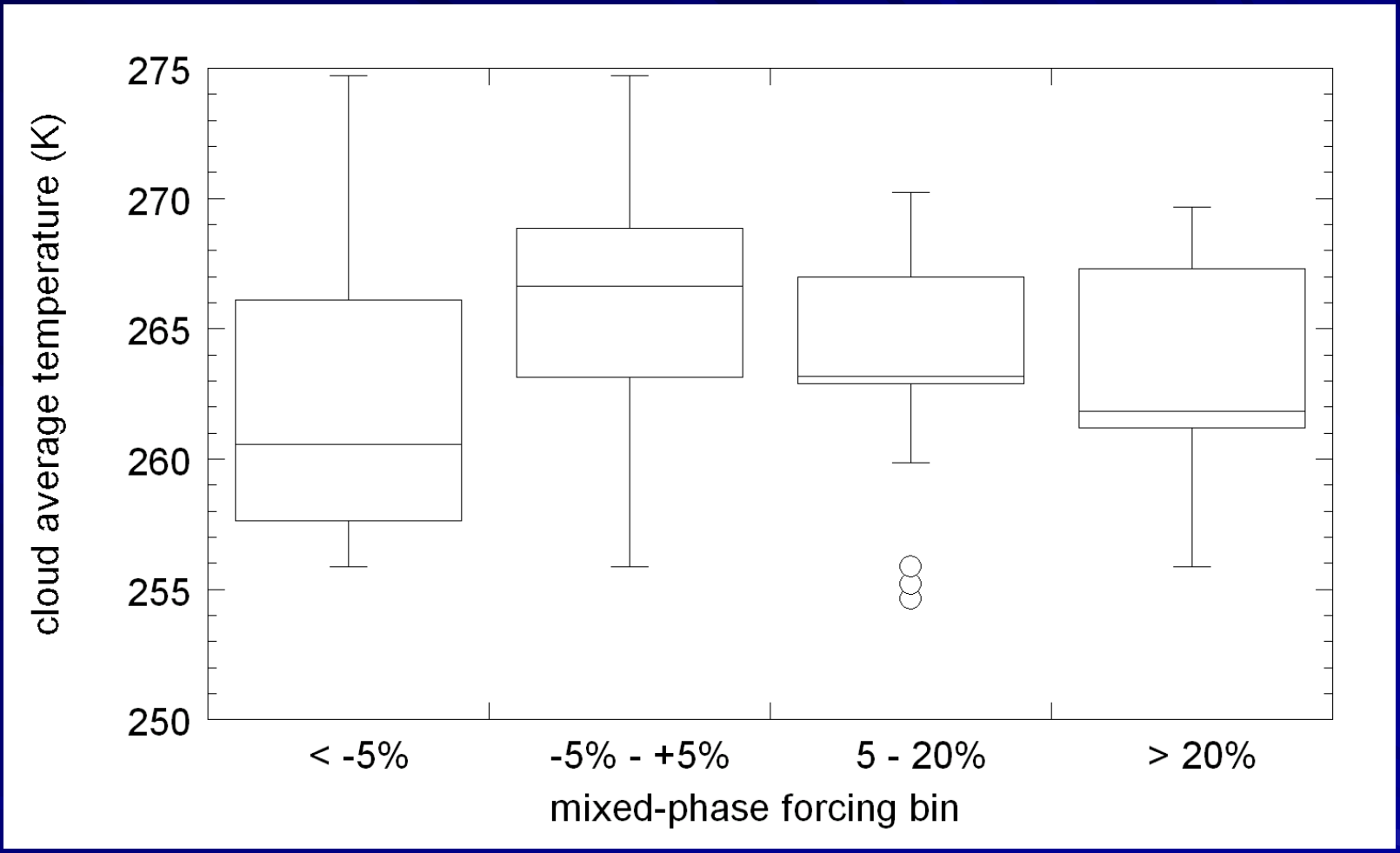

Figure 6. Box and whisker plot of average cloud temperature that prevailed during four general categories of mixed-phase surface forcing F_M described in the text. These data are taken only from within ±1 hr of the sonde launches. Plotting conventions are as in Figure 4.

Magnitude of Mixed Phase Forcing

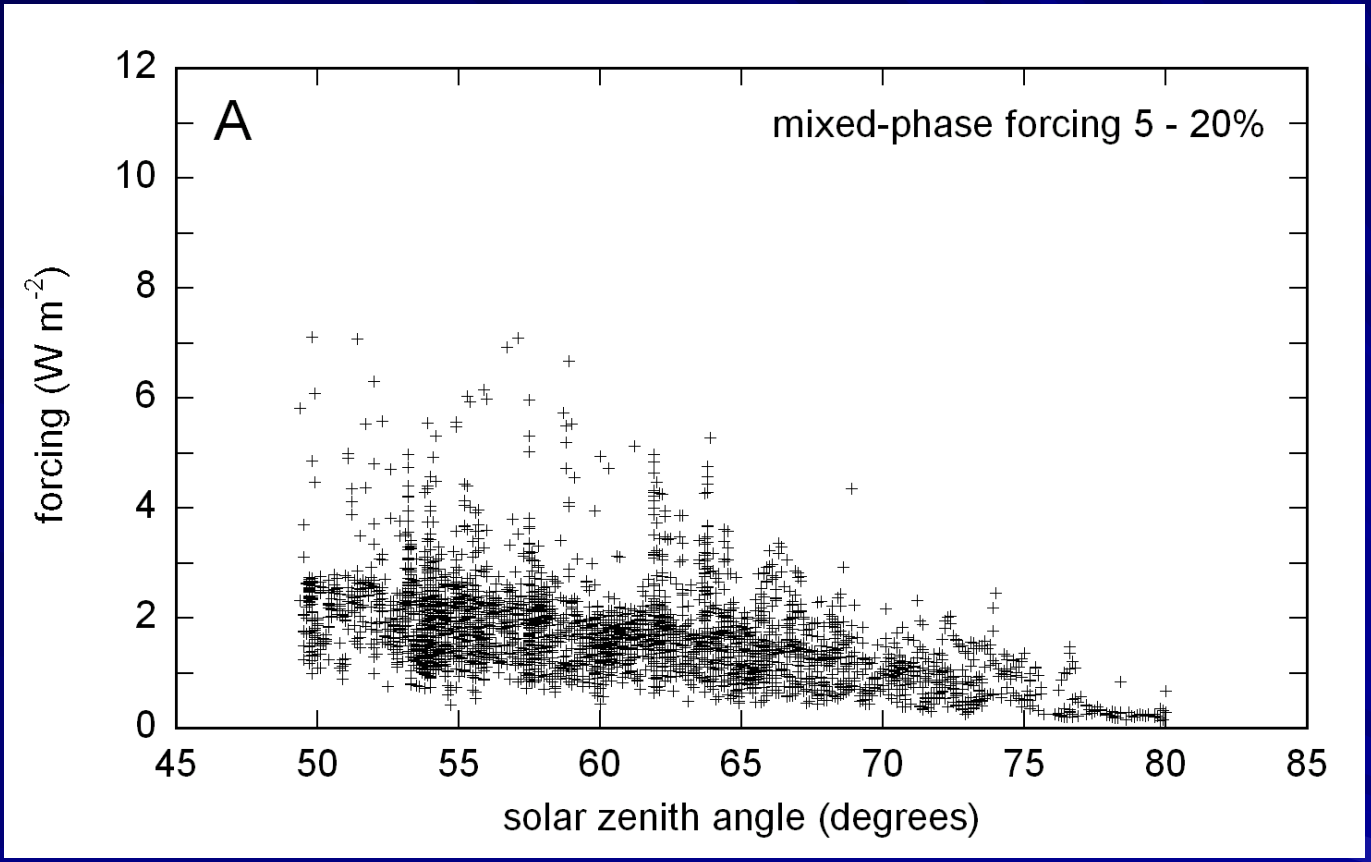

Figure 7. Mixed-phase surface forcing F_M in the 1.6-μm window as a function of solar zenith angle for all individual one-minute-averaged measurements: (A) for moderate *FM*; (B) for larger *FM*.

Magnitude of Mixed Phase Forcing

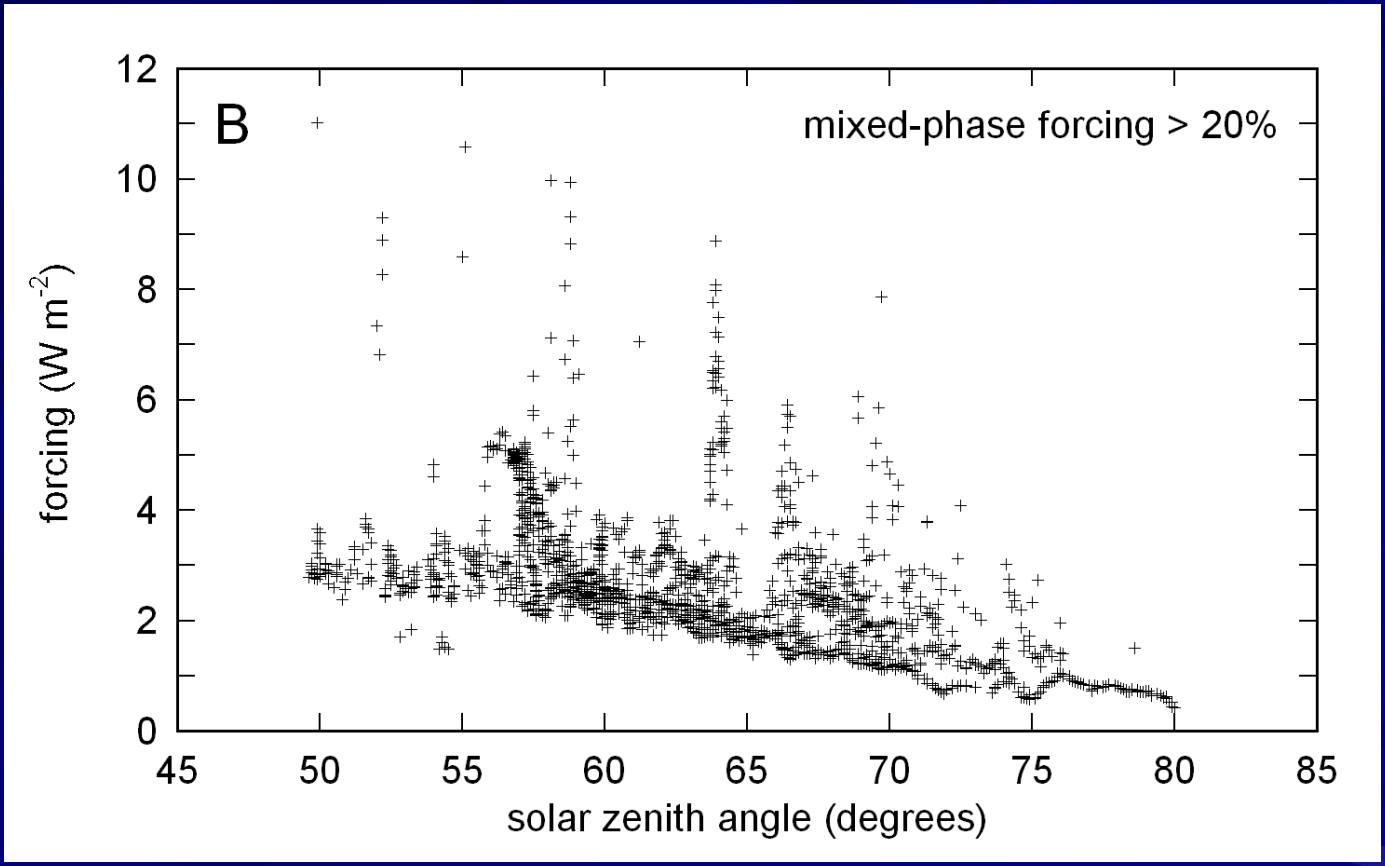

Figure 7. Mixed-phase surface forcing F_M in the 1.6-μm window as a function of solar zenith angle for all individual one-minute-averaged measurements: (A) for moderate *FM*; (B) for larger *FM*.

Distinguishing Small from Large Ice Particle Influences

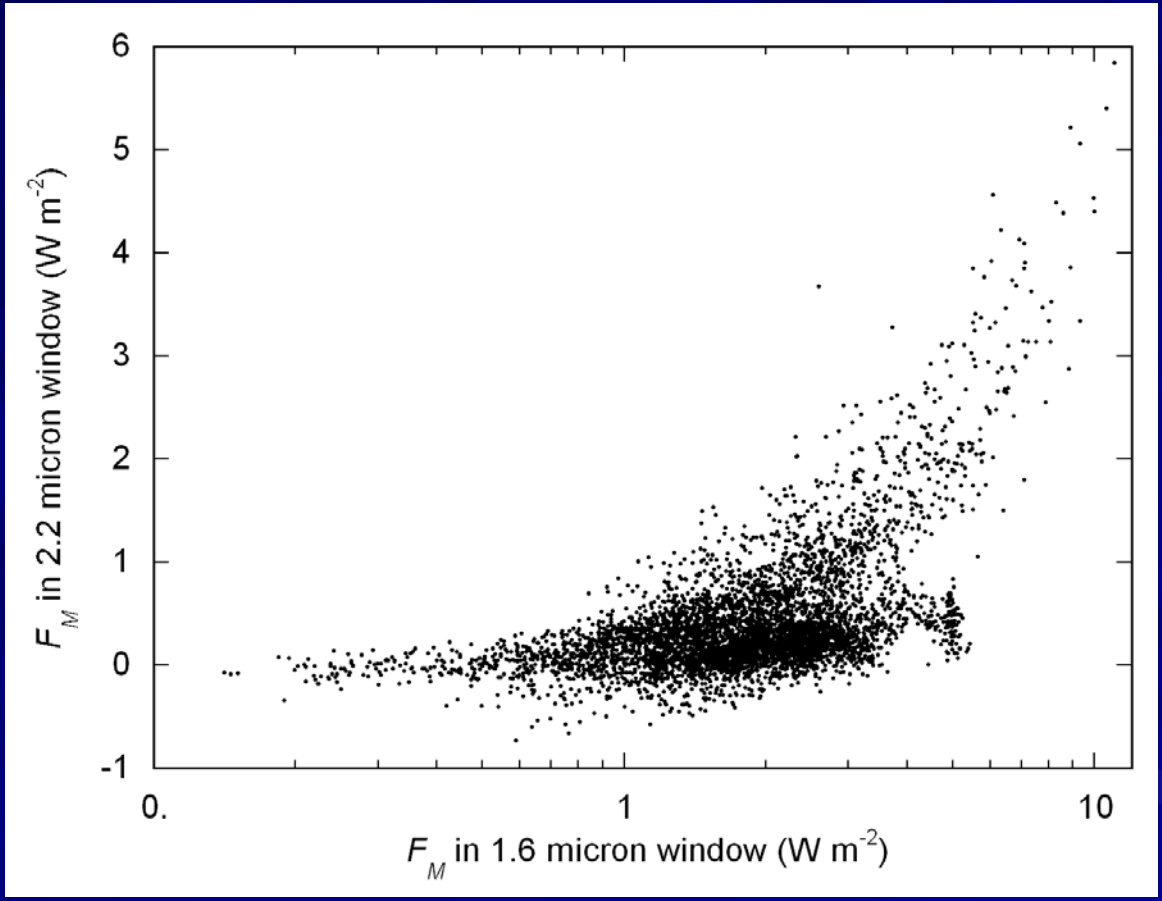

Figure 8. Mixed-phase surface forcing F_M in the 2.2 μm window as a function of F_M in the 1.6 μm window, plotted for all 1.6-μm $F_M \geq 5\%$ in the entire set of overcast sky retrievals.

Larger Ice Particles At Work

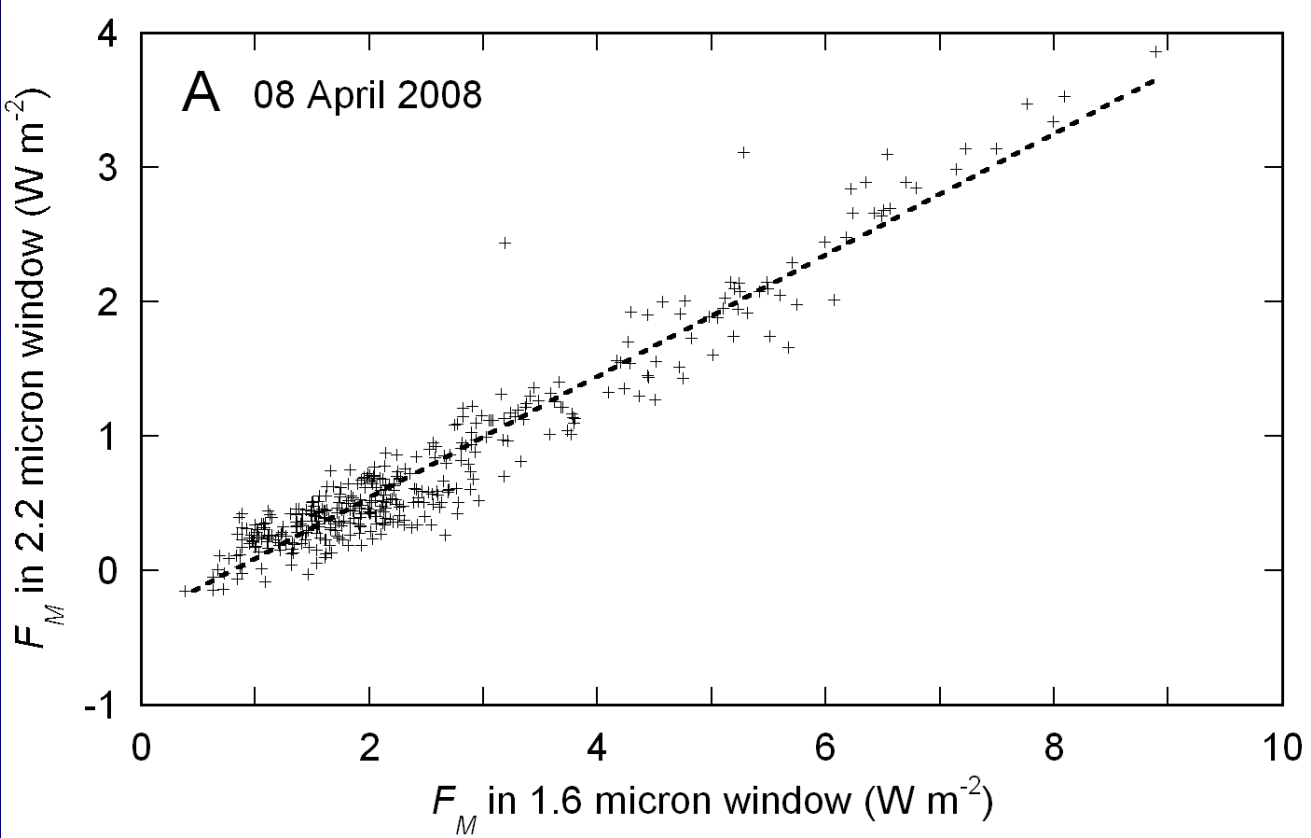

Figure 9. Mixed-phase surface forcing F_M in the 2.2 μm window as a function of F_M in the 1.6 μm window, plotted for all 1.6-μm $F_M \geq 5\%$ on specific days: (A) 8 April; (B) 26 April; (C) 19 April.

Larger Ice Particles At Work

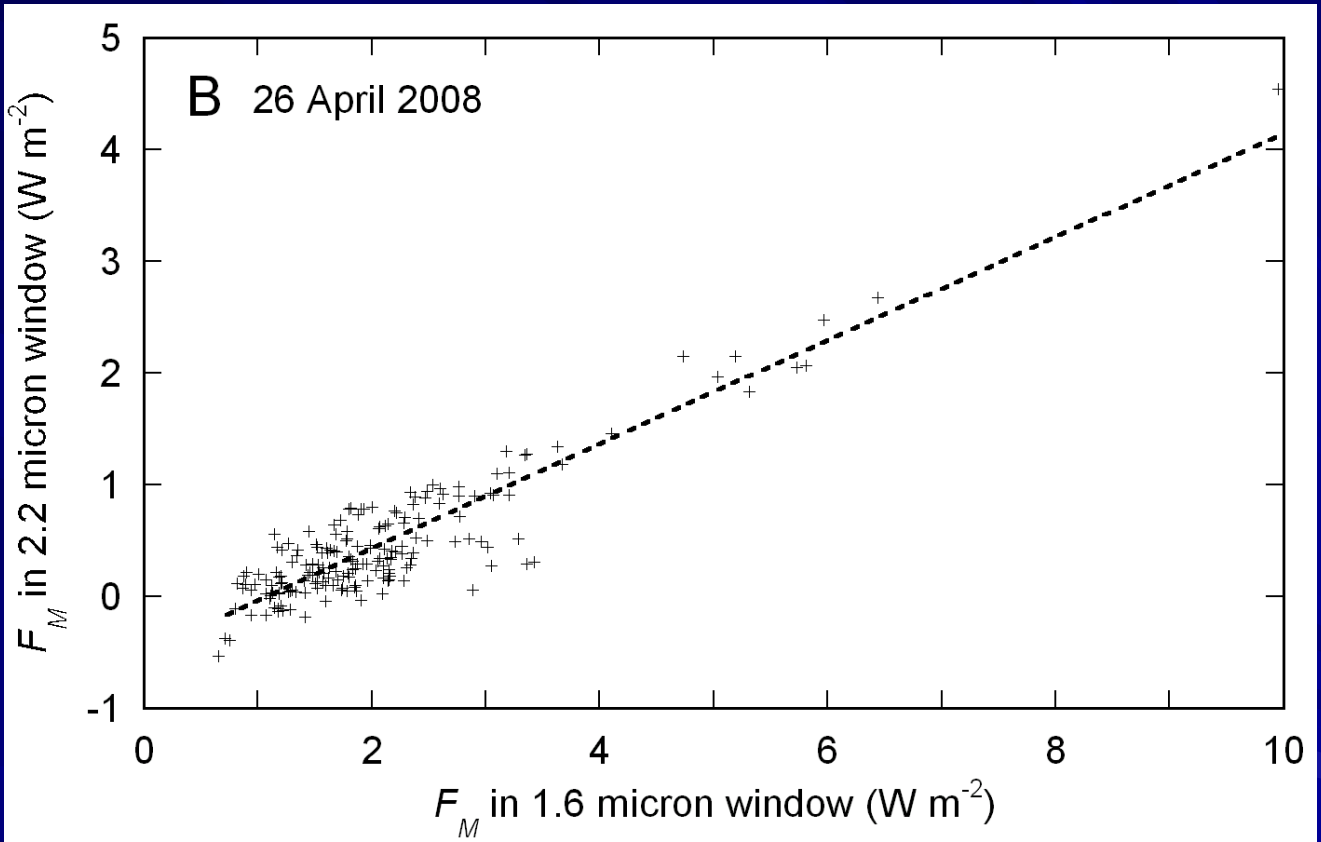

Smaller Ice Particles At Work